A Note on Bode Plot Asymptotes based on Transfer Function Coefficients

Young Chol Kim, Kwan Ho Lee and Young Tae Woo

School of Electrical & Computer Eng., Chungbuk National University, Cheongju 361-763, Korea
(Tel: +82-43-261-2475; Fax: +82-43-272-2475; Email:yckim@cbu.ac.kr)

Abstract: In this note, we present a different asymptotes from the standard approximate lines of the Bode magnitude plot. Wherein the pseudo break frequency is defined in terms of coefficients of denominator and numerator polynomials of the transfer function instead of its poles and zeros. Several comparative examples are given. This result can be used for the characteristic ratio assignment(CRA) [1], [2] with frequency response requirements, which is a method of designing linear controller in parameter space.

Keywords: Asymptotes, Bode magnitude plot, break frequency, characteristic ratio

1. Introduction

In the classical frequency response design using Bode plot, there are many cases that it is more convenient to use the asymptotes of frequency magnitude response and break point frequencies (which is sometimes called as corner frequency) instead of the exact Bode plots. In addition to the frequency response requirements, if we have to consider transient response specifications as like overshoot and the speed of response, the problem may not be easily carried out by using the conventional Bode plot. A reason is that the precise relationship between pole-zero locations of a system and its transient response is not yet known except for the case of a second order system. As different methods for directly dealing with time response problems, the characteristic ratio assignment [1], [2], [3] and the coefficient diagram method (CDM) [4] have been studied since the mid of 1990. These methods have been developed by expanding relationships between time response of an all pole system and the characteristic ratios and a generalized time constant, which are defined as functions of coefficients of transfer function. This idea was originally investigated by Naslin [5] in 1960 but has not been paid attention so much until Manabe [4] invented the CDM. It is important to note that (i) the characteristic ratios are closely related to the damping and the stability, and (ii) the speed of response is exactly characterized by the generalized time constant. Some of them have been proved recently by Kim [1]. It was shown in [1], [2], [3], [4] that the CRA and CDM are very useful for the problem of designing a controller that meets the time response requirements. First of all, it is remarkable that all the design procedures of CRA/CDM are carried out in parameter space. However, it is not adequate to apply both CRA/CDM directly to the design problem with frequency response specifications. In [5], Naslin also advocated that for a well damped all pole system, the points of intersection of the pseudo-asymptotes of its frequency magnitude are equal to the characteristic pulsatances. The pulsatances are defined by ratios of adjacent two coefficients of a polynomial. This is a simple method to draw an asymptotic gain diagram. Furthermore, this may be applied to the CRA and the CDM for the sake of considering the frequency response requirements. However, according to our observations, the pulsatances do not coincide with the real break points in the case of which the transfer function has either under-damped complex poles and zeros or multiple ones. In other words, when we use the pulsatances as pseudo break points, it must be restrictively applied to merely the well damped systems. This paper starts from this point. Consider a loop transfer function $L(s) = N(s)/D(s)$. From $|L(jw)|^2 = N(jw)N(-jw)/D(jw)D(-jw)$, each term of $|L(jw)|^2$ can be plotted separately. The modulus of the term in w gives a straight line of slope 1. Similarly, the term in w^k is represented by a straight line of slope k. We shall call these straight lines the pseudo asymptotes. Those lines intersect each other. Here the points of intersection are defined by new pseudo break points, which are finally represented in terms of the characteristic ratios and a generalized time constant of denominator and numerator polynomials individually. We will show through several comparative examples that the pseudo asymptotes coincide with real Bode plot for most cases of transfer functions. It is also shown that new pseudo break points are closely identical to the real corner frequencies well.

This research was supported in part by grant R01-2003-000-11738-0 from the Basic Research Program of the Korea Science & Engineering Foundation.

2. Asymptotes of Bode magnitude curve

In this section, we first give several definitions and then represent a new asymptote of the Bode magnitude plot.

2.1. Definitions and Motivation

The following definitions have been originally introduced by Naslin [5]. Consider a polynomial with real positive coefficients:

$$\delta(s) = \delta_n s^n + \delta_{n-1} s^{n-1} + \cdots + \delta_1 s + \delta_0, \quad \delta_i > 0. \tag{1}$$

The *characteristic ratios* are defined as:

$$\alpha_1 = \frac{\delta_1^2}{\delta_0 \delta_2}, \quad \alpha_2 = \frac{\delta_2^2}{\delta_1 \delta_3}, \quad \cdots, \quad \alpha_{n-1} = \frac{\delta_{n-1}^2}{\delta_{n-2} \delta_n} \tag{2}$$

and the *generalized time constant* is defined to be

$$\tau := \frac{\delta_1}{\delta_0}. \tag{3}$$

The *characteristic pulsatances* are defined by

$$\beta_0 = \frac{\delta_0}{\delta_1}, \quad \beta_1 = \frac{\delta_1}{\delta_2}, \quad \cdots, \quad \beta_{n-1} = \frac{\delta_{n-1}}{\delta_n} \tag{4}$$

Here this is called as *pulsatance* briefly. We then have

$$\alpha_1 = \frac{\beta_1}{\beta_0}, \quad \alpha_2 = \frac{\beta_2}{\beta_1}, \quad \cdots, \quad \alpha_n = \frac{\beta_n}{\beta_{n-1}} \tag{5}$$

The coefficients δ_i of $\delta(s)$ can also be represented in terms of α_i's and τ as follows:

$$\delta_1 = \delta_0 \tau \tag{6}$$

$$\delta_i = \frac{\delta_0 \tau^i}{\alpha_{i-1}\alpha_{i-2}^2\alpha_{i-3}^3 \cdots \alpha_2^{i-2}\alpha_1^{i-1}}, \quad \text{for } i = 2, \cdots, n. \tag{7}$$

We see that for a given set of values α_is, τ, and δ_0 the corresponding polynomial $\delta(s)$ is uniquely determined. As mentioned in introduction, all these parameters that are represented in terms of coefficients of the transfer function play very important roles in the CRA/CDM ([1], [4]). Naslin [5] has observed that the pulsatances of a well damped polynomial are closely identical to the real break frequencies of Bode plot. We give an example to show how the pulsatances relate to the the pseudo-asymptotes of frequency responses.

Example 1 Let us examine two cases: one is the well damped system and the other is not. Consider the following transfer function.

$$\begin{aligned} G(s) &= \frac{1}{(s/0.5+1)(s/2+1)(s/20+1)} \\ &= \frac{1}{0.05s^3 + 1.125s^2 + 2.55s + 1}. \end{aligned}$$

According to (4), pulsatances of the denominator are

$$\beta = [\beta_0 \quad \beta_1 \quad \beta_2] = [0.3922 \quad 2.2667 \quad 22.5].$$

It is seen that the pulsatances are very similar to the values of real break points of $G(s)$. We can also construct the corresponding transfer function with the pulsatances as follows:

$$G_p(s) = \frac{1}{(s/\beta_0+1)(s/\beta_1+1)(s/\beta_2+1)}.$$

As shown in Fig. 1, Bode plots of the $G(s)$ and $G_p(s)$ coincide with each other. Secondly, the following transfer function is the case including complex poles and zeros.

$$\begin{aligned} T(s) &= \frac{(s/10)^2 + 1.4s/10 + 1}{(s/0.5+1)(s/3+1)[(s/50)^2 + 0.8(s/50) + 1]} \\ &= \frac{0.01s^2 + 0.14s + 1}{2.667 \cdot 10^{-4}s^4 + 0.0116s^3 + 0.7044s^2 + 2.3493s + 1}. \end{aligned}$$

The pulsatances of numerator and denominator of $T(s)$ are

$$\begin{aligned} \text{Numerator}: \ & [\beta_0^N \quad \beta_1^N] = [7.1492 \quad 14] \\ \text{Denominator}: \ & [\beta_0^D \quad \beta_1^D \quad \beta_2^D \quad \beta_3^D] = [0.426 \quad 3.335 \quad 43.5 \quad 60.724] \end{aligned}$$

Constructing the transfer function whose poles and zeros are equal to β_i^N and β_j^D, it becomes

$$T_p(s) = \frac{(s/\beta_0^N+1)(s/\beta_1^N+1)}{(s/\beta_0^D+1)(s/\beta_1^D+1)(s/\beta_2^D+1)(s/\beta_3^D+1)}.$$

Bode plots of $T(s)$ and $T_p(s)$ are shown in Fig. 2. There are some errors near complex modes between $T(s)$ and $T_p(s)$.

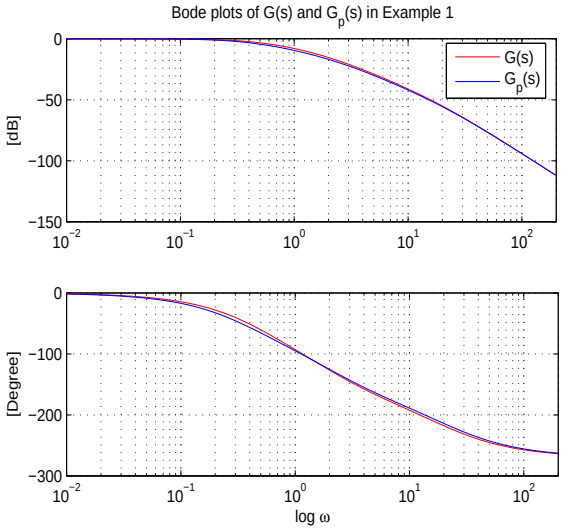

Fig. 1. Bode plots of $G(s)$ and $G_p(s)$ in Example 1.

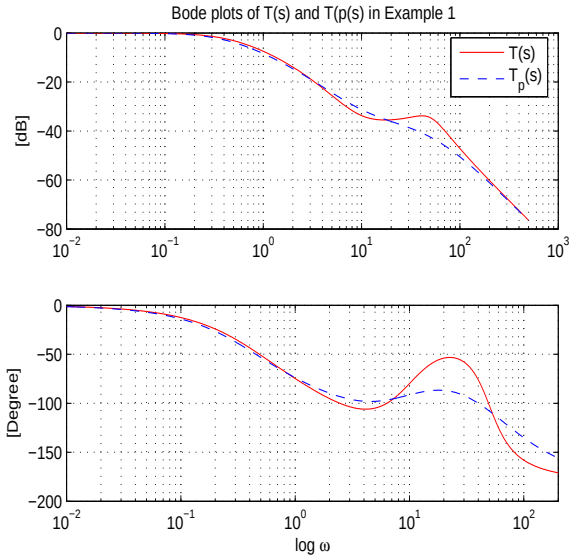

Fig. 2. Bode plots of $T(s)$ and $T_p(s)$ in Example 1.

This difference becomes larger in the case where the complex poles and zeros are closely placed. ♣

In [4], [5],they have addressed that the pulsatances are very useful for drawing the approximate frequency response plot and then can be applied to the design procedure like the CDM although it may have large error in some cases. Because the pulsatances are ratio of two adjacent coefficients of polynomial, it is very easy to tune the controller parameters so that meets the given frequency requirements. However, if the plant has poor damping, the design approach based on the pulsatances may result in unsatisfactory controller due to large approximation error.

2.2. New pseudo-break frequency

Now, we represent a new pseudo-break frequency. As the first step to proceed this, let us consider the following all

pole transfer function of order n.

$$G(s) = \frac{N(s)}{D(s)} = \frac{a_0}{a_n s^n + a_{n-1}s^{n-1} + \cdots + a_1 s + a_0}. \quad (8)$$

The frequency magnitude can be given by

$$\begin{aligned} |G(j\omega)|^2 = & \quad G(j\omega)G(-j\omega) \\ = & \quad \frac{a_0^2}{c_n^2\omega^{2n} + c_{n-1}^2\omega^{2(n-1)} + \cdots + c_1^2\omega^2 + c_0^2}. \end{aligned} \quad (9)$$

Taking the logarithm on both sides of (9), it becomes

$$log(|G(j\omega)|) = log(a_0) - log(|D(j\omega)|), \quad (10)$$

where

$$log|D(j\omega)| = \frac{1}{2} log(c_n^2\omega^{2n} + c_{n-1}^2\omega^{2(n-1)} + \cdots + c_1^2\omega^2 + c_0^2). \quad (11)$$

Here we define the asymptote of (11) as follows:

$$log|D(j\omega)| \approx log|D(j\omega)|_p := log|c_0| + log|c_1\omega| + \cdots + log|c_n\omega^n|. \quad (12)$$

Every terms in right hand side of (12) are straight lines with slopes $0, 1, 2, \cdots$, which we will call the *pseudo-asymptotes*. The unit of this slope is $6[dB/Oct]$ or $20[dB/Dec]$. Then the intersection of each two adjacent lines is defined as the *pseudo-break frequency*. From (12)

$$\omega_{p0} := \frac{c_0}{c_1}, \quad \omega_{p1} := \frac{c_1}{c_2}, \quad \cdots, \quad \omega_{pn-1} := \frac{c_{n-1}}{c_n}. \quad (13)$$

The following Example 2 shows pseudo-break frequencies and pseudo-asymptotes of an all pole transfer function.

Example 2 Consider the following transfer function.

$$\begin{aligned} G(s) = \frac{N(s)}{D(s)} &= \frac{545}{(s+1)(s+5)(s+10+j3)(s+10-j3)} \\ &= \frac{545}{s^4 + 26s^3 + 234s^2 + 754s + 545}. \end{aligned}$$

Then we have

$$\begin{aligned} c_0 = a_0 = 545, \quad c1 = -2a_2a_0 + a_1^2 = 559.87, \\ c_2 = 2a_0 + a_2^2 - 2a_3a_1 = 128.99, \\ c_3 = a_3^2 - 2a_2 = 14, 42, \quad c_4 = 1. \end{aligned}$$

Using (13), we obtain the pseudo-break points.

$$[\omega_{p0}\ \omega_{p1}\ \omega_{p2}\ \omega_{p3}] = [0.97\ \ 4.34\ \ 8.94\ \ 14.42].$$

We see that the pseudo-break frequencies are very similar to the real break points. The pseudo-break frequencies and the pseudo-asymptotes have been depicted in Fig. 3 where

$$|G_k| := 20log(a_0) - 20log|c_k\omega^k|, \quad k = 0, 1, \cdots, 4. \quad \clubsuit$$

Now our problem is to express the pseudo-break points in terms of characteristic ratios and pulsatances. Recall the all pole system in (8) and (9).

$$|G(j\omega)|^2 = \frac{a_0^2}{D(j\omega)D(-j\omega)} = \frac{1}{\overline{Q}^2(\omega)} \quad (14)$$

Define

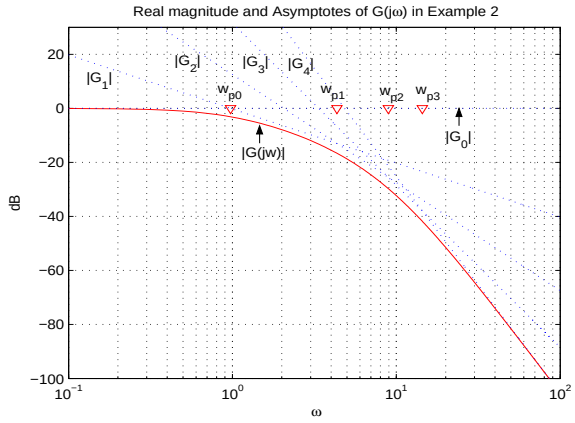

Fig. 3. Real magnitude curve and asymptotes of $G(s)$ in Example 2.

$$\Delta_i^j := \begin{cases} \Pi_{k=i,i<j}^{j}\alpha_k, & \text{if } 0 < i < j \\ \alpha_i, & \text{if } 0 < i = j. \end{cases} \quad (15)$$

Using (6), (7), and (15),

$$\begin{aligned} \overline{Q}^2(\omega) \ = \ & 1 + \eta_1\tau^2\omega^2 + \frac{\eta_2\tau^4}{\left(\Delta_1^1\right)^2}\omega^4 + \frac{\eta_3\tau^6}{\left(\Delta_1^1\Delta_1^2\right)^2}\omega^6 + \cdots \\ & + \frac{\eta_n\tau^{2n}}{\left(\Delta_1^1\Delta_1^2\Delta_1^3\cdots\Delta_1^{n-1}\right)^2}\omega^{2n} \end{aligned} \quad (16)$$

where

$$\begin{aligned} \eta_k : \ = \ & 1 - \frac{2}{\alpha_k} + \frac{2}{\alpha_k\Delta_{k-1}^{k+1}} - \frac{2}{\alpha_k\Delta_{k-1}^{k+1}\Delta_{k-2}^{k+2}} + \cdots \\ & + (-1)^k \frac{2}{\alpha_k\Pi_{j=1}^{k-1}\Delta_{k-j}^{k+j}}. \end{aligned} \quad (17)$$

If we draw the approximated curve of $|G(j\omega)|$ vs. frequency by plotting each term in (16) with pseudo-asymptotes, a typical shape is as shown in Fig. 4.

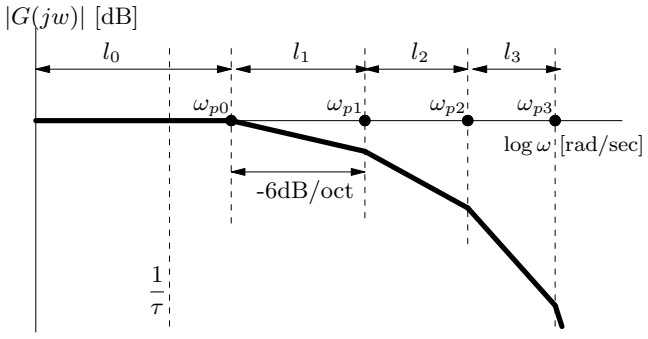

Fig. 4. Pseudo-asymptotic diagram of $|G(j\omega)|$.

From (11) and (13), the pseudo-break points in (16)are identical to

$$\omega_{pi} := \sqrt{\frac{\eta_i}{\eta_{i+1}}} \cdot \frac{\Delta_1^i}{\tau}, \quad i = 0, 1, \cdots, n-1. \quad (18)$$

where $\eta_0 = 1$ and $\Delta_1^0 = 1$. Let

$$l_i := \log\omega_{pi} - \log\omega_{p(i-1)}, \quad (19)$$

then we may write

$$l_0 = -\left(\log\tau + \frac{1}{2}\log\eta_1\right) \quad (20)$$

$$l_i = \log\eta_i - \frac{1}{2}(\log\eta_{i-1} + \log\eta_{i+1}) + \log\alpha_i, \quad (21)$$
$$where \quad i = 1, 2, \cdots, n-1.$$

Remark 1 It has been observed from eq.(17) that $\eta_i \approx \eta_{i+1}$ for $i = 1, 2, \cdots, n-1$ as α_i increases sufficiently larger than 2. Under this condition, then $l_i \approx \log\alpha_i$ and $\omega_{pi} < \omega_{p(i+1)}$ for all i. It results that the pseudo break points ω_{pi} lie in the form of sequential line-up. Since the time domain responses of a strictly proper system are dominantly related to the frequency magnitude at lower frequency than that of which the magnitude has about $-20[db]$, we know that three values of l_0, l_1, l_2 and l_3 play a significant role in the responses. Consequently, α_1, α_2, α_3 and τ have much greater influence than the rest. Indeed, α_1, α_2 and α_3 are the most dominant factors dictating the size of overshoot while τ can be used approximately to consider bandwidth or speed of response [6]. ♣

The main concept of pseudo-break frequency that has been introduced for all pole transfer function so far can be extended to the general case. Let us consider $N(s)$ of degree m. Since $|G(j\omega)|^2 = \frac{N(j\omega)N(-j\omega)}{D(j\omega)D(-j\omega)}$, we have

$$log(|G(j\omega)|) = log(|N(j\omega)|) - log(|D(j\omega)|), \quad (22)$$

where $log(|D(j\omega)|)$ is the same as (11) and

$$log|N(j\omega)| = \frac{1}{2}log(f_m^2\omega^{2m} + f_{m-1}^2\omega^{2(m-1)} + \cdots + f_1^2\omega^2 + f_0^2). \quad (23)$$

Then we can define the asymptote of (22) as follows:

$$\begin{aligned} log|G(j\omega)| \approx log|G(j\omega)|_p &:= log|N(j\omega)|_p - log|D(j\omega)|_p \\ &= \{log|f_0| + log|f_1\omega| + \cdots + log|f_m\omega^m|\} \\ &\quad -\{log|c_0| + log|c_1\omega| + \cdots + log|c_n\omega^n|\}. \end{aligned} \quad (24)$$

The pseudo-break points of numerator are separately defined in the similar way as those of denominator.

3. Comparative examples

In this section, we will give several examples to evaluate the proximity of new pseudo-break frequency and pseudo-asymptotes by comparing with the real values. The nearness of pulsatances defined by Naslin will be also compared with true systems in the same examples.

Example 3 (The case of no zero and distinct, real poles) Consider the all pole transfer function $T_1(s)$ with unit DC gain whose poles are

$$-0.5,\ -3,\ -15,\ -50,\ -100,\ -300,\ -500$$

Real break points, pseudo-break point and pulsatances of this transfer function are provided in Table 1. Fig. 5 shows their Bode magnitude curves. It is seen that Both break points and asymptotes closely approximate the actual values in this well damped case. ♣

Table 1. Different break frequencies of $T_1(j\omega)$ in Ex. 3.

k	real break points(ω_k)	pseudo-break points(ω_{pk})	pulsatances (β_k)
1	0.5	0.493	0.41
2	3	2.976	2.684
3	15	14.49	12.2
4	50	46.15	39.67
5	100	104.99	108.12
6	300	275.94	302.15
7	500	593.91	968.5

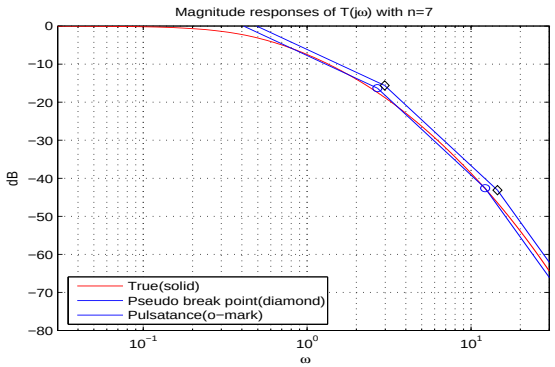

Fig. 5. Bode magnitude plots and asymptotes of $T_1(s)$ in Ex. 3.

Example 4 (The case of no zero and three real plus two pairs of complex poles) Consider the following transfer function

$$T_2(s) = \frac{7.134\ 10^7}{(s+2)(s+10)(s+30)(s^2+16s+164)(s^2+50s+725)}.$$

Real break points, pseudo-break point and pulsatances of $T_2(s)$ are provided in Table 2. Fig. 6 shows their Bode magnitude curves. We can see through Table 2 and Fig. 6 that the pseudo-break points and pseudo-asymptotes approximate more closely than those of pulsatances in this case. ♣

Table 2. Different break frequencies of $T_2(j\omega)$ in Ex. 4.

k	real break points(ω_k)	pseudo-break points(ω_{pk})	pulsatances (β_k)
1	2	1.96	1.25
2	10	9.41	4.22
3	12.81	9.92	8.29
4	12.81	16.46	14.02
5	26.93	19.02	24.05
6	26.93	27.99	44.82
7	30	44.52	108

Example 5 (The case of no zero and 7 poles distributed around a circle in s-plane) Consider the transfer function $T_3(s)$ with unit DC gain whose poles are

$$-10.405,\ -7.3495 \pm j7.3649,\ -9.5887 \pm j4.039,$$
$$-4.9236 \pm j9.1659 \quad .$$

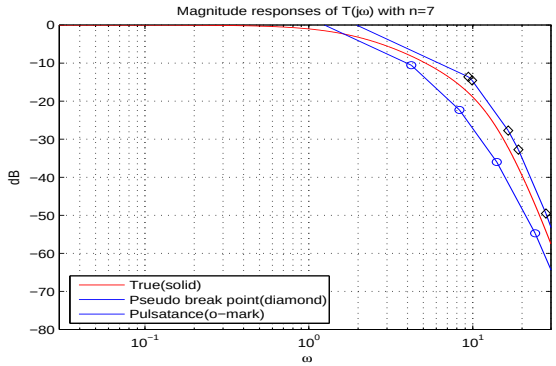

Fig. 6. Bode magnitude plots and asymptotes of $T_2(s)$ in Ex. 4.

The pole locations of $T_3(s)$ are depicted in Fig. 7. Real break points, pseudo-break point and pulsatances of $T_3(s)$ are provided in Table 3. Fig. 8 shows their Bode magnitude curves. We can see through Table 3 and Fig. 8 that the pseudo-break points and pseudo-asymptotes approximate much more closely than those of pulsatances in this case. ♣

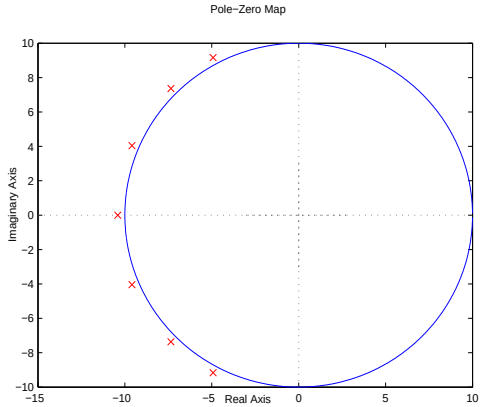

Fig. 7. Pole diagram of $T_3(s)$ in Ex. 5.

Table 3. Different break frequencies of $T_3(j\omega)$ in Ex. 5.

k	real break points(ω_k)	pseudo-break points(ω_{pk})	pulsatances (β_k)
1	10.405	8.94	2
2	10.405	9.165	4.2
3	10.405	9.622	6.857
4	10.405	10.405	10.405
5	10.405	11.25	15.79
6	10.405	11.81	425.78
7	10.405	12.11	54.13

Example 6 (The case of 3 zeros and 7 poles) Here we consider a transfer function $T_4(j\omega)$ including three zeros with unit DC gain. Its zeros and poles are

$$\text{Zeros}: \quad -6, \quad -15 \pm j10$$
$$\text{Poles}: \quad -2, \quad -10, \quad -30, \quad -8 \pm j10, \quad -25 \pm j10.$$

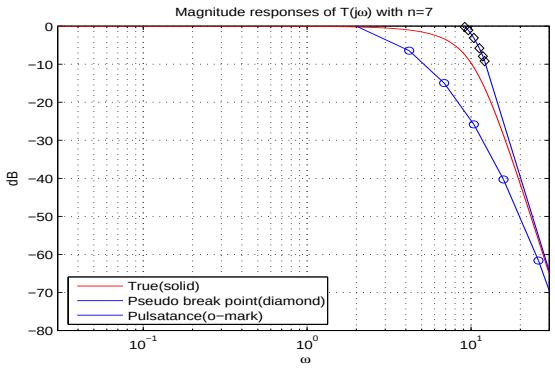

Fig. 8. Bode magnitude plots and asymptotes of $T_3(s)$ in Ex. 5.

As shown in Table 4 and Fig. 9, the pseudo break frequencies and pseudo-asymptotes result in satisfactory approximation. However, the error between real values and those by pulsatances over the middle frequency range are significantly larger than 3 $[dB]$. This is also verified by the Bode plots of three transfer functions which are generated on the basis of pseudo-break points and pulsatances respectively as shown in Fig. 10. ♣

Table 4. Different break frequencies of $T_4(j\omega)$ in Ex. 6.

	k	real break points(ω_k)	pseudo-break points(ω_{pk})	pulsatances (β_k)
Num.	1	6	5.76	3.86
	2	18.03	16.91	14.03
	3	18.03	20.02	36
Den.	1	2	1.96	1.25
	2	10	9.406	4.22
	3	12.806	9.922	8.29
	4	12.806	16.462	14.02
	5	26.926	19.016	24.05
	6	26.926	27.99	44.824
	7	30	44.52	108

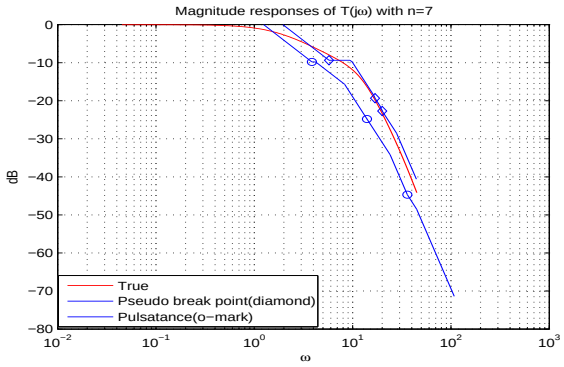

Fig. 9. Bode magnitude plots and asymptotes of $T_4(s)$ in Ex. 6.

4. Concluding remark

In the standard Bode plot, the break points between asymptotic straight lines are composed of poles and zeros of the transfer function. As like the usefulness of parametric stability criteria [4], [7], if there are any methods that will be able

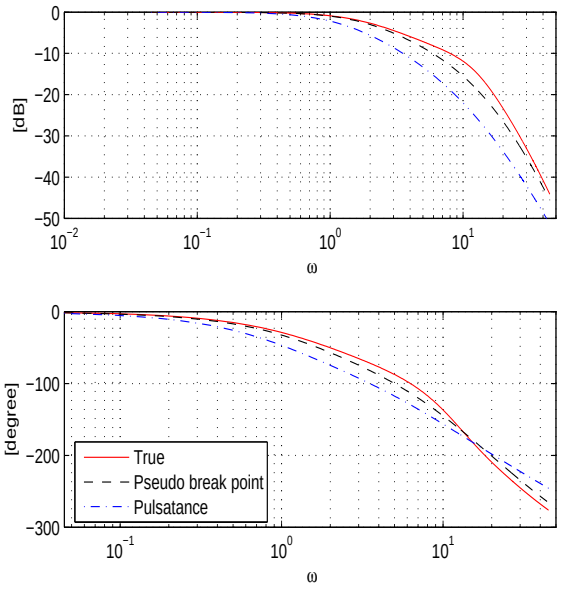

Fig. 10. Bode plots of $T_4(s)$, $T_{4pseudo}(s)$, $T_{4pulsa}(s)$ in Ex. 6.

to estimate the break points directly from the coefficients of transfer function instead of roots, such methods will be very useful for some classical controller design problems with frequency performance specifications. For the sake of this purpose, we have introduced a new pseudo-break point which is defined in terms of only the coefficients of transfer function. Through comparative studies of the pseudo-break point and the pulsatance defined by Naslin, it has been showed that the approximation errors by the pseudo-break points are not larger than about 3 $[dB]$ and that the proposed one provides much more effective approximation than that of the pulsatance. However, the pulsatance is easier to use than the pseudo-break point in applications since it is simply defined by the ratio of adjacent two coefficients.

References

[1] Y.C. Kim, L.H. Keel, and S.P. Bhattacharyya, "Transient response control via characteristic ratio assignment," *IEEE Trans. on Automatic Control*, vol. AC-48, no.12, pp.2238-2244, Dec. 2003.

[2] Y.C. Kim, L.H. Keel, and S. Manabe, "Controller design for time domain specification," *Proc. of 2002 IFAC World Congress*, Barcelona, Spain, July, 2002.

[3] K.S. Kim, Y.C. Kim, L.H. Keel, and S.P. Bhattacharyya, "PID controller design with time response specifications," *Proc. of 2003 American Control Conf.*, Denver, USA, June, 2003.

[4] S. Manabe, "Coefficient diagram method", *Proc. of the 14th IFAC Symp. on Automatic Control in Aerospace*, pp.199-210, Seoul, Korea, 1998.

[5] P. Naslin, *Essentials of Optimal Control*, Boston Technical Publishers, Inc., 1969.

[6] Youngchol Kim, Keunsik Kim and S. Manabe, "Sensitivity of time response to characteristic ratios," *Proc. of 2004 American Control Conf.*, pp.2723-2728, Boston, USA, June, 2004.

[7] S.P. Bhattqacharyya, H. Chapellat and L.H. Keel, *Robust Control: The Parametric Approach*, Prentice Hall Inc., 1995.